


Communication

# Synthesis of Porous Organic Polymers with Tunable Amine Loadings for CO<sub>2</sub> Capture: Balanced Physisorption and Chemisorption

Xueying Kong <sup>1,2</sup>, Shangsiying Li <sup>1</sup>, Maria Strømme <sup>2</sup>  and Chao Xu <sup>1,2,\*</sup>

<sup>1</sup> Key Laboratory of Flexible Electronics (KLOFE), Institute of Advanced Materials (IAM), Nanjing Tech University (Nanjing Tech), 30 South Puzhu Road, Nanjing 211800, China

<sup>2</sup> Division of Nanotechnology and Functional Materials, Department of Engineering Sciences, Uppsala University, SE-75121 Uppsala, Sweden

\* Correspondence: chao.xu@angstrom.uu.se

Received: 1 July 2019; Accepted: 13 July 2019; Published: 17 July 2019



**Abstract:** The cross-coupling reaction of 1,3,5-triethynylbenzene with terephthaloyl chloride gives a novel ynone-linked porous organic polymer. Tethering alkyl amine species on the polymer induces chemisorption of CO<sub>2</sub> as revealed by the studies of ex situ infrared spectroscopy. By tuning the amine loading content on the polymer, relatively high CO<sub>2</sub> adsorption capacities, high CO<sub>2</sub>-over-N<sub>2</sub> selectivity, and moderate isosteric heat ( $Q_{st}$ ) of adsorption of CO<sub>2</sub> can be achieved. Such amine-modified polymers with balanced physisorption and chemisorption of CO<sub>2</sub> are ideal sorbents for post-combustion capture of CO<sub>2</sub> offering both high separation and high energy efficiencies.

**Keywords:** porous organic polymers; amine modification; CO<sub>2</sub> separation; adsorption mechanism; chemisorption of CO<sub>2</sub>

## 1. Introduction

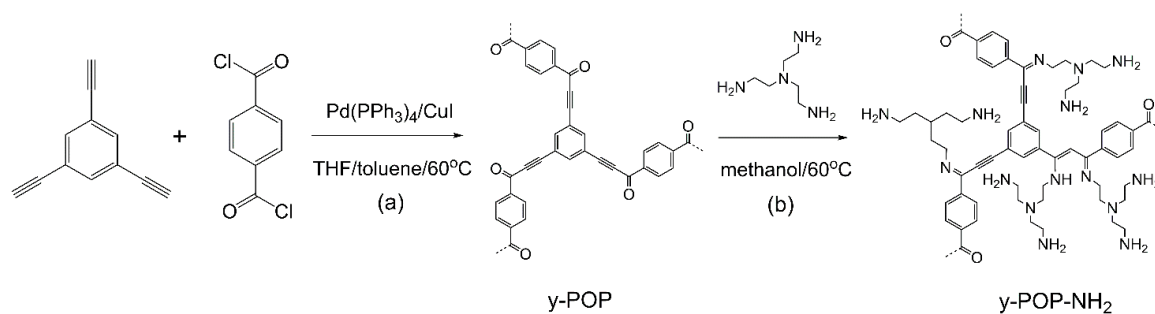
The long-term increasing CO<sub>2</sub> emission from combustion of fossil fuels is widely considered as the main reason for the global climate change and associated environmental issues [1]. Post-combustion carbon capture dealing with separation of CO<sub>2</sub> from flue gases is a feasible approach to reduce industrial CO<sub>2</sub> emissions and to gain control over the atmospheric CO<sub>2</sub> concentration, and the method has the advantage of allowing quite simple retrofit design of required instrumentation into existing power plants [2]. However, the main challenge for the post-combustion technology is that the low concentration of CO<sub>2</sub> (ca. 5%–15 v%) in flue gases usually results in low separation efficiency [3]. Amine scrubbing, a mature technique using aqueous amine solution to absorb CO<sub>2</sub> from mixed gases, has been applied in natural gas purification and CO<sub>2</sub> capture for more than a half century [4] and the technique is currently employed to create large scale pilot facilities in, amongst others, Norway [5]. The strong chemical interactions between amine and CO<sub>2</sub> molecules endow the high efficiency for CO<sub>2</sub> capture and separation. However, the energy consumption for amine reactivation arising from heating the aqueous amine solution is high. In addition, the use of amine might cause amine leakage and serious corrosion to the equipment. Therefore, it is highly desirable to develop new materials for post-combustion carbon capture that can be operated in an economical and environmentally friendly manner.

Porous materials with high surface areas and high volumes of narrow pores are ideal solid sorbents for adsorption-driven CO<sub>2</sub> capture, in which CO<sub>2</sub> molecules can be selectively adsorbed onto the surface or captured in the narrow pores [6,7]. For example, traditional zeolites and activated carbons have been extensively studied for CO<sub>2</sub> capture owing to their high microporosities and relatively high

CO<sub>2</sub> adsorption capacities [8–14]. However, the hydrophilicity of zeolites and the broad pore size distributions of activated carbons have significantly limited their performances in CO<sub>2</sub> capture and separation. Emerging porous materials such as metal–organic frameworks (MOFs) [15–17] and porous organic polymers (POPs) [18–23] are of great interest for CO<sub>2</sub> capture because of their large surface areas and tunable pore sizes. POPs constitute a type of porous materials created by linking pure organic monomers, usually aromatic or conjugated, via strong covalent bonds [24,25]. The diverse synthesis possibilities of POPs allows precise control of their nanoporous structure and surface chemistry at the molecular level, aiming to increase the CO<sub>2</sub> adsorption capacity and selectivity of CO<sub>2</sub> over other gases by thermodynamic effects [26–31]. Several studies reported on post-modification of POPs with alkyl amines for CO<sub>2</sub> capture [32–39]. The strong CO<sub>2</sub>–amine interactions on the amine-modified POPs led to significantly enhanced CO<sub>2</sub> adsorption capacity and increased CO<sub>2</sub>-over-N<sub>2</sub> selectivity. However, the strong interactions, interpreted by the high isosteric heat ( $Q_{st}$ ) of adsorption (up to 80 kJ mol<sup>-1</sup>) [35,37], require high energy input to reactivate the sorbents in the process of temperature swing adsorption (TSA) or vacuum swing adsorption (VSA) [40]. In this context, it would be great of interest to balance the trade-off between the separation efficiency and energy efficiency. Here, we report a strategy to tune the amine density on a novel ynone-linked POP (y-POP) by the post-modification approach, which enables balancing of the effects of physisorption and chemisorption of CO<sub>2</sub> and optimization of the CO<sub>2</sub> adsorption capacity, CO<sub>2</sub>-over-N<sub>2</sub> selectivity and heat of adsorption of CO<sub>2</sub>.

## 2. Results and Discussion

POPs can be synthesized from various organic reactions, of which coupling reactions constitute the most commonly used routes [41]. For example, Zhu et al. reported on the Yamamoto homo-coupling reaction of tetrakis(4-bromophenyl)methane for the synthesis of a porous aromatic framework (PAF-1) [42]. The tetrahedral shaped monomer resulted in a three-dimensional framework of PAF-1 possessing an ultrahigh surface area of 5600 m<sup>2</sup> g<sup>-1</sup>. Cooper and Jiang's groups synthesized a number of conjugated microporous polymers (CMPs) by Suzuki, Sonogashira, and Glaser coupling reactions, which showed great potential in photocatalysis, light harvesting, etc. [43–46]. Recently, Son et al. developed a carbonylative Sonogashira coupling reaction of phenyl alkynes and phenyl halides in the presence of carbon monoxide, which gave a redox-active CMP that can be used as electrode material for electrochemical energy storage devices [47]. Therefore, the exploration of organic reactions to form novel structures in POPs could enrich their properties and applications. As we know, the cross-coupling reaction between terminal alkynes and acyl chloride under Sonogashira conditions forms conjugated  $\alpha,\beta$ -alkynic ketones, also known as ynones [48]. More interestingly, further reaction of the ynones with alkyl amines could form imine compounds by two possible routes [48–52]. One is that of conjugate addition of the amine to  $\alpha,\beta$ -alkynic ketone with formation of enamionone, which can be further converted into the imine compound via the nucleophilic addition in the presence of excess of amine. Another approach is direct nucleophilic addition of the amine to the ketone group forming the imine or enamionone compound. However, to the best of our knowledge, the direct coupling of terminal alkyne with acyl chloride has never been reported for the synthesis of POPs. In this context, we attempted the cross-coupling of 1,3,5-triethynylbenzene with terephthaloyl chloride under Sonogashira conditions for the synthesis of y-POP, which was catalyzed by bis(triphenylphosphine)palladium(II) dichloride and copper(I) iodide in the presence of trimethylamine as a base (Scheme 1a). The conjugated structure of the ynones and the aromatic monomers endow rigidity and stability of y-POP. In order to graft amine species onto the polymer, the as-synthesized y-POP was treated by tris(2-aminoethyl)amine (**tren**) in a methanol solution (Scheme 1b). The density of amine species tethered on the polymer was finely controlled by tuning the concentration of **tren** in the methanol solution. Specifically, treatment of y-POP in the methanol solution of **tren** (1, 5, 20 v%) yields the amine modified polymer y-POP-NH<sub>2</sub>, denoted as y-POP-A1, y-POP-A2, and y-POP-A3, respectively. Based on the thermogravimetric analyses (Figure S1), the amine loading content on the y-POP-NH<sub>2</sub> can be roughly calculated to 12%, 16%, and 19% for y-POP-A1, y-POP-A2, and y-POP-A3, respectively.



**Scheme 1.** (a) Synthesis of ynone-linked porous organic polymer (y-POP) by the Sonogashira coupling reaction; (b) amine modification of y-POP.

The molecular structures of y-POP and y-POP-NH<sub>2</sub> were examined by both Fourier transform infrared (IR) and solid-state <sup>13</sup>C nuclear magnetic resonance (NMR) spectroscopy. The IR spectrum of y-POP shows strong bands at 2200 and 1720 cm<sup>-1</sup>, corresponding to the stretching vibrations of alkyne (–C≡C–) and carbonyl (–C=O), respectively (Figure 1a). In general, the central –C≡C– group with a high degree of symmetry displays a very weak IR stretching band [45]; however, the intensity of the IR band can be significantly increased by introducing conjugated structures [47,53]. Therefore, the intense IR band observed for the alkyne group can be correlated to the formation of conjugated structure with a carbonyl group (–C≡C(=O)–). The study of the solid-state <sup>13</sup>C NMR spectrum also confirms the formation of ynone species in the polymer. The bands at chemical shifts of 91 and 83 ppm can be assigned to carbon atoms (1, 2) of alkyne bonds (Figure 1b and Figure S2). The characteristic band for carbon atoms (3) in carbonyl groups was observed at 176 ppm. Upon amine modification, the intensity of the IR band at 1720 cm<sup>-1</sup> was gradually decreased with increasing amine loading, indicating that the carbonyl groups were consumed by the amine. In addition, the IR band intensity at 2200 cm<sup>-1</sup> and NMR band intensity at 91 and 83 ppm were decreased in y-POP-NH<sub>2</sub> compared to y-POP due to the transformation of the alkyne groups to enaminones. The broad shoulder bands at ~1660 cm<sup>-1</sup> in the IR spectra of y-POP-NH<sub>2</sub> can be assigned to the imine stretching vibrations. Consistently, the broad shoulder bands at the NMR chemical shift of 175–168 ppm for y-POP-NH<sub>2</sub> indicate the formation of enamine and imine bonds [52,54]. The broad IR bands at 3370 cm<sup>-1</sup> observed for y-POP-NH<sub>2</sub> are assigned to the characteristic N–H stretching modes for the primary amine. The chemical shifts at 52 and 39 ppm for y-POP-NH<sub>2</sub> correspond to the carbons in tethered **tren** species. The three major peaks at 137, 130 and 123 ppm are assigned to the aromatic carbons in y-POP and y-POP-NH<sub>2</sub>. Other peaks in the range of 60–10 ppm can be assigned to the carbon atoms in solvent molecules (tetrahydrofuran, methanol, triethylamine) adsorbed in the pores of y-POP. Collectively, the studies of the IR and <sup>13</sup>C NMR spectra confirmed that ynone-linked POP was successfully synthesized and the **tren** molecules were chemically tethered on y-POP-NH<sub>2</sub>.

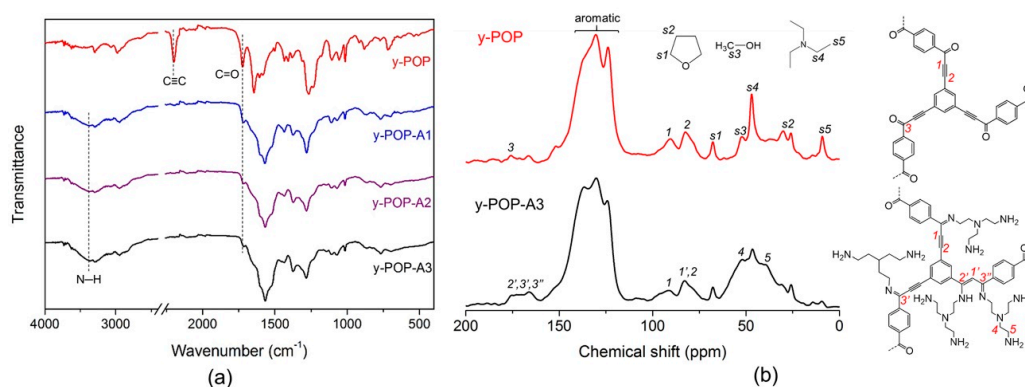


**Figure 1.** (a) Infrared (IR) and (b) <sup>13</sup>C nuclear magnetic resonance (NMR) spectra of ynone-linked porous organic polymer (y-POP) and y-POP-NH<sub>2</sub>.

As a strong organic base with a  $pK_b$  value  $\approx 4$ , the tethered **tren** species on *y*-POP-NH<sub>2</sub> could potentially attract CO<sub>2</sub> molecules by the chemisorption effect. To investigate the CO<sub>2</sub> adsorption mechanism, we designed an *ex situ* IR experiment to study the molecular interactions between CO<sub>2</sub> and the polymers. The polymer sample was grinded with KBr and pressed into a transparent pellet, followed by drying at 100 °C for 12 h. The degassed pellet was used to record the IR background spectrum in a transmission model. The pellet was subsequently flashed with CO<sub>2</sub> for 2 h at room temperature and thereafter a transmission IR spectrum was recorded again. The differences between the two spectra revealed the adsorbed CO<sub>2</sub> on the polymers, as shown in Figure 2. The intense bands at frequencies of 2335 and 653 cm<sup>-1</sup> in the spectra correspond to the physisorbed CO<sub>2</sub> molecules, which can be assigned to the asymmetric stretching and deformation vibration of C=O, respectively [55]. Physisorption clearly dominates the CO<sub>2</sub> adsorption on *y*-POP as no extra band was observed in the IR spectrum. In contrast, significant IR bands in the frequency region of 1750–1000 cm<sup>-1</sup> were observed for *y*-POP-NH<sub>2</sub>, which indicates that the tethered amine species induced chemisorption of CO<sub>2</sub>. Obviously, a higher amine loading content in *y*-POP-NH<sub>2</sub> resulted in a stronger IR intensity, suggesting the enhanced effect of chemisorption of CO<sub>2</sub>. The band at the frequency of 1704 cm<sup>-1</sup> was assigned to C=O stretching (amide I), which is a characteristic indication of the formation of carbamic acid or carbamate species from the reaction between CO<sub>2</sub> and the amine groups on *y*-POP-NH<sub>2</sub> [56–58]. The broad band at 1243 cm<sup>-1</sup> was assigned to a combination of N–H bending and C–N stretching (amide III) [59]. In addition, the bands at 1655, 1618, and 1475 cm<sup>-1</sup> can be assigned to asymmetric deformation of NH<sub>3</sub><sup>+</sup> and the signals at 1538 and 1385 cm<sup>-1</sup> can be associated to asymmetric stretching of COO<sup>-</sup> [55,60–63]. Therefore, we could speculate that chemisorption of CO<sub>2</sub> on *y*-POP-NH<sub>2</sub> forms ammonium carbamate ion pairs (Scheme S1).

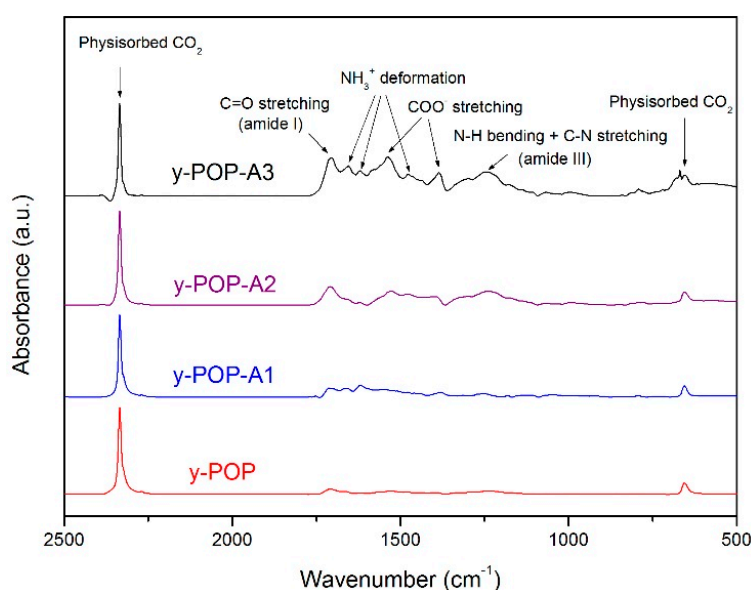


**Figure 2.** Infrared (IR) spectra of adsorbed CO<sub>2</sub> on ynone-linked porous organic polymer (*y*-POP) and *y*-POP-NH<sub>2</sub>.

The porosities of the polymers were analyzed by N<sub>2</sub> sorption measurements at 77 K, as illustrated in Figure 3a. The sorption isotherm of *y*-POP displays rapid N<sub>2</sub> adsorption at low relative pressures ( $p/p_0 < 0.05$ ), which is characteristic for microporous materials. The significant N<sub>2</sub> uptake at high relative pressures ( $p/p_0 > 0.8$ ) and the accompanied hysteresis loop between the adsorption and desorption branches suggest the presence of mesopores in *y*-POP arising from the inter-particle cavities observed in SEM images (Figure S3). Such mesopores would facilitate the mass transportation and increase the adsorption kinetics during the sorption processes. Pore size distribution analyses showed that *y*-POP had ultramicropores (pore size: 0.74 nm), micropores (pore size: 1.2 nm) and mesopores (pore size:

34 nm). As expected, amine modification on y-POP resulted in disappearance of the ultramicropores and decrease in both micropore volumes and total pore volumes due to the pore blocking effect of the **tren** species (Figure 3b). Consistently, the specific surface area of the y-POP-NH<sub>2</sub> was gradually decreased with increasing amine loading: the specific surface area values being 226, 145, 107, and 84 m<sup>2</sup> g<sup>-1</sup>, for of y-POP, y-POP-A1, y-POP-A2, and y-POP-A3, respectively.

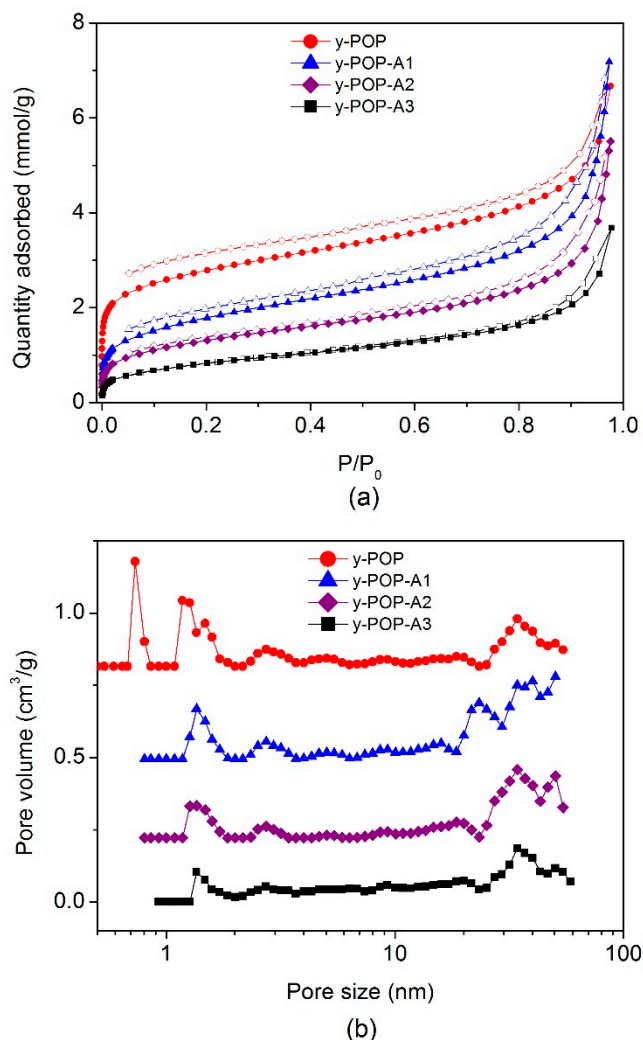


**Figure 3.** (a) N<sub>2</sub> adsorption/desorption isotherms of ynone-linked porous organic polymer (y-POP) and y-POP-NH<sub>2</sub> recorded at 77 K; (b) Pore size distribution analyses of y-POP and y-POP-NH<sub>2</sub> based on the adsorption branches using the density functional theory model.

Given the microporous structure and the strong chemisorption of CO<sub>2</sub> induced by the high amount of amine species, we anticipated that y-POP-NH<sub>2</sub> would have much higher CO<sub>2</sub> adsorption capacities and higher CO<sub>2</sub>-over-N<sub>2</sub> selectivity than the corresponding values of unmodified y-POP. Figure 4a compares the CO<sub>2</sub> adsorption isotherms of y-POP and y-POP-NH<sub>2</sub> with different amine densities at 273 K. Although the specific surface areas of the polymers were reduced after the amine modification, y-POP-NH<sub>2</sub> had significantly higher CO<sub>2</sub> adsorption capacities than the substrate polymer of y-POP. With the increase of amine loading, the CO<sub>2</sub> adsorption capacity of y-POP-NH<sub>2</sub> gradually increased up to 1.11 and 1.88 mmol g<sup>-1</sup> at 0.15 and 1 bar (273 K), respectively, which were 158% and 40% higher than the corresponding values of y-POP (0.43 mmol g<sup>-1</sup> at 0.15 bar; 1.34 mmol g<sup>-1</sup> at 1 bar, 273 K). In addition, the sorbents can be easily reactivated and showed excellent adsorption recyclability. For example, y-POP-A1 retained 97% of its CO<sub>2</sub> adsorption capacity after 5 cycles at 293 K (Figure S6). In order to evaluate the potential of the polymers for capturing CO<sub>2</sub> from flue gases, we calculated the

CO<sub>2</sub>-over-N<sub>2</sub> selectivity from their single component adsorption data recorded at 273 K (Figure 4a and Figure S7) using ideal adsorption solution theory (IAST) [13,35,64,65]. The CO<sub>2</sub> and N<sub>2</sub> adsorption isotherms were fitted by dual-site and single-site Langmuir equation, respectively (Figure S8 and Table S1). The CO<sub>2</sub>-over-N<sub>2</sub> selectivity is defined as  $S = (x_{CO_2}/y_{CO_2})/(x_{N_2}/y_{N_2})$ , where  $x$  and  $y$  are the molar fractions of the gas in the adsorbed and bulk phases, respectively. A simulated gas mixture of 15 v% CO<sub>2</sub>/85 v% N<sub>2</sub> was used for the calculation. As illustrated in Figure 4b, the substrate polymer y-POP showed a relatively low CO<sub>2</sub>-over-N<sub>2</sub> selectivity of 20. In contrast, y-POP-NH<sub>2</sub> containing amine species displayed much higher selectivity up to  $4.15 \times 10^3$ . In addition, we have calculated Henry's law initial slope selectivity for the polymers (Figure S9), which are comparable to the values obtained from the IAST calculations.

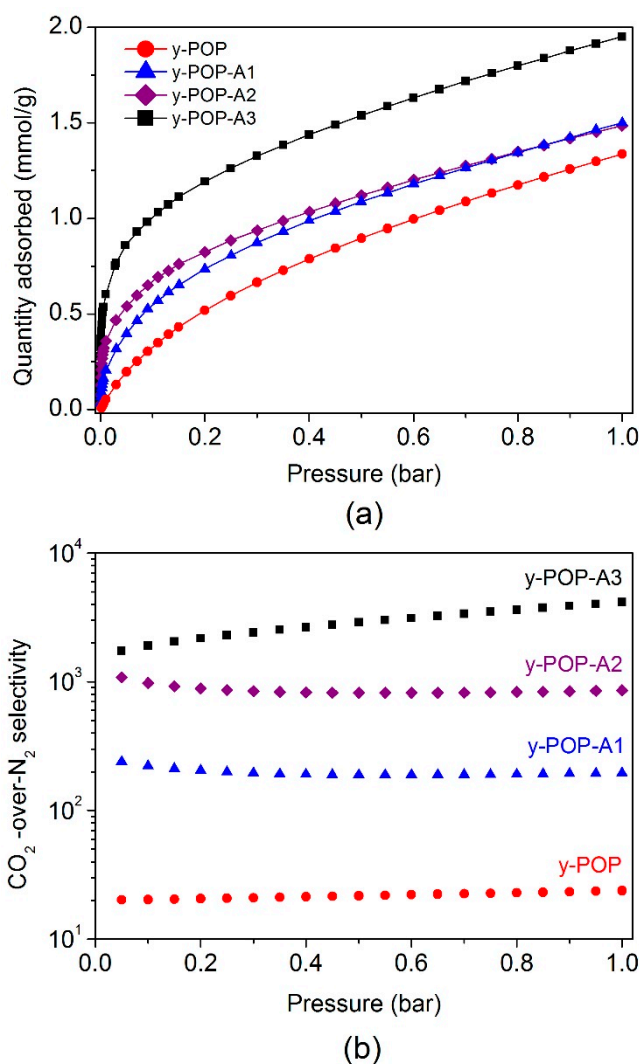


**Figure 4.** (a) CO<sub>2</sub> adsorption isotherms of ynone-linked porous organic polymer (y-POP) and y-POP-NH<sub>2</sub> with different amine loadings at 273 K; (b) CO<sub>2</sub>-over-N<sub>2</sub> selectivity of y-POP and y-POP-NH<sub>2</sub> calculated by ideal adsorbed solution theory.

The binding affinity of the studied polymers toward CO<sub>2</sub> was revealed by the  $Q_{st}$  values, which can be calculated from the temperature dependent CO<sub>2</sub> adsorption isotherms (273, 283, and 293 K) using the Clausius–Clapeyron equation. The substrate polymer of y-POP had a relatively low  $Q_{st}$  value of 29.0 kJ mol<sup>-1</sup>, which is characteristic for the physisorption of CO<sub>2</sub>. As expected, y-POP-NH<sub>2</sub> showed gradually increased  $Q_{st}$  values (y-POP-A1: 46.8 kJ mol<sup>-1</sup>; y-POP-A2: 62.2 kJ mol<sup>-1</sup>; y-POP-A3:

76.5 kJ mol<sup>-1</sup>) with increasing amine loading (Figure S5). The high  $Q_{st}$  values indicate the effect of chemisorption of CO<sub>2</sub> on y-POP-NH<sub>2</sub>, which is consistent with the ex situ IR results.

Table 1 summarizes CO<sub>2</sub> adsorption capacities, CO<sub>2</sub>-over-N<sub>2</sub> selectivity, and  $Q_{st}$  values for the four studied polymers. It is immediately clear that amine modification on the polymer significantly increases the efficiency for CO<sub>2</sub> capture and separation due to the effect of chemisorption of CO<sub>2</sub>. In addition, the efficiency was proportional to the amine loading density on the polymer. However, the polymers containing high amine loading contents had relatively high  $Q_{st}$  values, which means that reactivation of the sorbents requires a high energy consumption. Noteworthy, the sample y-POP-A1 had relatively high CO<sub>2</sub> adsorption capacities (0.65 mmol g<sup>-1</sup> at 0.15 bar; 1.50 mmol g<sup>-1</sup>; 273 K) and high CO<sub>2</sub>-over-N<sub>2</sub> selectivity of 271 (273 K). The selectivity is comparable to some top-performing sorbents of amine-modified POPs [32], MOFs [66] and silica [67] that indicates the potential of using y-POP-A1 for efficient CO<sub>2</sub> capture. In contrast, y-POP-A1 demonstrates a moderate  $Q_{st}$  value of 46.8 kJ mol<sup>-1</sup> at a low coverage of CO<sub>2</sub> (0.2 mmol g<sup>-1</sup>), which is much lower than those of amine-modified sorbents (mmen-CuBTTri: 96 kJ mol<sup>-1</sup>; [66] PP1-2-tren: 80 kJ mol<sup>-1</sup>; [37] NTU-1: 75 kJ mol<sup>-1</sup>; [35] PEI (40 wt%) ⊂ PAF-5: 68.7 kJ mol<sup>-1</sup> [38]; PPN-6-CH<sub>2</sub>-TETA: 63 kJ mol<sup>-1</sup> [32]). Therefore, the balanced effects of physisorption and chemisorption of CO<sub>2</sub> on y-POP-A1 would offer both high separation efficiency and high energy efficiency for post-combustion capture of CO<sub>2</sub> from flue gases.

**Table 1.** A summary of specific surface area ( $S_{BET}$ ), CO<sub>2</sub> adsorption capacity (273 K), CO<sub>2</sub>-over-N<sub>2</sub> selectivity (273 K), and  $Q_{st}$  of CO<sub>2</sub> adsorption at the low coverage of CO<sub>2</sub> for ynone-linked porous organic polymer (y-POP) and y-POP-NH<sub>2</sub> with different amine densities.

Sample	Amine Loading	$S_{BET}$ (m <sup>2</sup> g <sup>-1</sup> )	CO <sub>2</sub> Uptake (mmol g <sup>-1</sup> )		CO <sub>2</sub> /N <sub>2</sub> Selectivity		$Q_{st}$ (kJ mol <sup>-1</sup> )
			0.15 bar	1 bar	IAST	Henry's Law	
y-POP	0	226	0.43	1.34	20	22	29.0
<b>y-POP-A1</b>	<b>12%</b>	<b>145</b>	<b>0.65</b>	<b>1.50</b>	<b>239</b>	<b>216</b>	<b>46.8</b>
y-POP-A2	16%	107	0.76	1.49	1083	750	62.2
y-POP-A3	19%	84	1.11	1.95	4154	3806	76.5

### 3. Conclusions

To conclude, a novel ynone-linked POP was synthesized and its molecular structure was fully characterized by IR and <sup>13</sup>C NMR spectroscopy. The polymer was further used as a substrate to tether alkyl amine species by post modification. The ex situ IR results revealed that the amine species on the polymers could induce chemisorption of CO<sub>2</sub> with formation of ammonium carbamate ion pairs. As a result, the amine-modified polymers showed high CO<sub>2</sub> adsorption capacities, high CO<sub>2</sub>-over-N<sub>2</sub> selectivity, as well as high  $Q_{st}$  values. Remarkably, the amine density on the polymers can be finely controlled by a molecular engineering approach, which allows balancing the physisorption and chemisorption of CO<sub>2</sub> to reach a high separation efficiency, excellent recyclability, high energy efficiency for CO<sub>2</sub> capture and separation. The use of this strategy in the design of amine-modified porous solids (e.g., mesoporous silica, MOFs, clay, etc.) would offer highly efficient sorbents for post-combustion capture of CO<sub>2</sub>.

**Supplementary Materials:** The following are available online at <http://www.mdpi.com/2079-4991/9/7/1020/s1>. Figure S1. Thermogravimetric analysis curves of y-POP and y-POP-NH<sub>2</sub>. Figure S2. Solid-state <sup>13</sup>C NMR spectra of y-POP, y-POP-A1, y-POP-A2, and y-POP-A3. Figure S3. SEM images of y-POP, y-POP-A1, y-POP-A2, and y-POP-A3. Figure S4. Powder X-ray diffraction patterns of y-POP and y-POP-NH<sub>2</sub> showing the polymers are mainly amorphous. Figure S5. CO<sub>2</sub> adsorption isotherms of y-POP, y-POP-A1, y-POP-A2, and y-POP-A3 recorded at 293 K. Figure S6. CO<sub>2</sub> adsorption-desorption cycles for y-POP-A1 recorded at 293 K. Figure S7. N<sub>2</sub> adsorption isotherms of y-POP, y-POP-A1, y-POP-A2, and y-POP-A3 recorded at 273 K. Figure S8. CO<sub>2</sub> (■) and N<sub>2</sub> (▲) adsorption data and of y-POP and y-POP-NH<sub>2</sub> recorded at 273 K. The red solid lines show the fitting results of the data: The CO<sub>2</sub> and N<sub>2</sub> adsorption data was fitted by a dual-site and single-site Langmuir model, respectively. Detail fitting results are given in Table S1. The fitted parameters from the single adsorption data were used to predict the IAST selectivity. Figure S9. The CO<sub>2</sub> and N<sub>2</sub> adsorption data of (a) y-POP, (b) y-POP-A1, (c) y-POP-A2, and (d) y-POP-A3 at low partial pressures at 273 K and the linearly fitted results. Henry's law CO<sub>2</sub>-over-N<sub>2</sub>

selectivities were calculated from the initial slopes of the CO<sub>2</sub> and N<sub>2</sub> isotherms. Table S1. Fitting parameters for the CO<sub>2</sub> and N<sub>2</sub> adsorption data recorded at 273 K. Scheme S1. Possible mechanism of chemisorption of CO<sub>2</sub> on y-POP-NH<sub>2</sub> with high amine loadings.

**Author Contributions:** X.K. and S.L. contributed equally to this work. Synthesis and characterization: X.K., S.L., C.X.; Data analysis: X.K., S.L., M.S., and C.X.; Writing: M.S. and C.X.

**Funding:** This research was funded by the Åforsk research grant, STINT (The Swedish Foundation for International Cooperation in Research and Higher Education) initiation grant, the Natural Science Foundation of Jiangsu Province (BK20170994), and the Natural Science Fund for Colleges and Universities in Jiangsu Province (17KJB430018).

**Acknowledgments:** We thank Samson Afewerki for valuable discussions.

**Conflicts of Interest:** The authors declare no conflict of interest.

## References

1. *Climate Change 2014: Synthesis Report; Contribution of Working Groups I, II and III to the Fifth Assessment Report of the Intergovernmental Panel on Climate Change; IPCC: Geneva, Switzerland, 2014.*
2. Haszeldine, R.S. Carbon Capture and Storage: How Green Can Black Be? *Science* **2009**, *325*, 1647–1652. [CrossRef]
3. Agarwal, A.; Biegler, L.T.; Zitney, S.E. A superstructure-based optimal synthesis of PSA cycles for post-combustion CO<sub>2</sub> capture. *AIChE J.* **2010**, *56*, 1813–1828. [CrossRef]
4. Rochelle, G.T. Amine scrubbing for CO<sub>2</sub> capture. *Science* **2009**, *325*, 1652–1654. [CrossRef]
5. CCS in Norway Entering a New Phase. Available online: <https://www.gassnova.no/en/ccs-in-norway-entering-a-new-phase> (accessed on 29 June 2018).
6. D'Alessandro, D.M.; Smit, B.; Long, J.R. Carbon Dioxide Capture: Prospects for New Materials. *Angew. Chem. Int. Ed.* **2010**, *49*, 6058–6082. [CrossRef]
7. Samanta, A.; Zhao, A.; Shimizu, G.K.H.; Sarkar, P.; Gupta, R. Post-Combustion CO<sub>2</sub> Capture Using Solid Sorbents: A Review. *Ind. Eng. Chem. Res.* **2012**, *51*, 1438–1463. [CrossRef]
8. Chue, K.T.; Kim, J.N.; Yoo, Y.J.; Cho, S.H.; Yang, R.T. Comparison of Activated Carbon and Zeolite 13X for CO<sub>2</sub> Recovery from Flue Gas by Pressure Swing Adsorption. *Ind. Eng. Chem. Res.* **1995**, *34*, 591–598. [CrossRef]
9. Zhao, J.; Xie, K.; Singh, R.; Xiao, G.; Gu, Q.; Zhao, Q.; Li, G.; Xiao, P.; Webley, P.A. Li+/ZSM-25 Zeolite as a CO<sub>2</sub> Capture Adsorbent with High Selectivity and Improved Adsorption Kinetics, Showing CO<sub>2</sub>-Induced Framework Expansion. *J. Phys. Chem. C* **2018**, *122*, 18933–18941. [CrossRef]
10. Jiang, Y.; Ling, J.; Xiao, P.; He, Y.; Zhao, Q.; Chu, Z.; Liu, Y.; Li, Z.; Webley, P.A. Simultaneous biogas purification and CO<sub>2</sub> capture by vacuum swing adsorption using zeolite NaUSY. *Chem. Eng. J.* **2018**, *334*, 2593–2602. [CrossRef]
11. Sethia, G.; Sayari, A. Comprehensive study of ultra-microporous nitrogen-doped activated carbon for CO<sub>2</sub> capture. *Carbon* **2015**, *93*, 68–80. [CrossRef]
12. Sevilla, M.; Mokaya, R.; Al-Jumaily, A.S.M.; Fuertes, A.B. Optimization of the Pore Structure of Biomass-Based Carbons in Relation to Their Use for CO<sub>2</sub> Capture under Low- and High-Pressure Regimes. *ACS Appl. Mater. Interfaces* **2018**, *10*, 1623–1633. [CrossRef]
13. Xu, C.; Ruan, C.-Q.; Li, Y.; Lindh, J.; Strømme, M. High-Performance Activated Carbons Synthesized from Nanocellulose for CO<sub>2</sub> Capture and Extremely Selective Removal of Volatile Organic Compounds. *Adv. Sustain. Syst.* **2018**, *2*, 1700147. [CrossRef]
14. Xu, C.; Strømme, M. Sustainable Porous Carbon Materials Derived from Wood-Based Biopolymers for CO<sub>2</sub> Capture. *Nanomaterials* **2019**, *9*, 103. [CrossRef]
15. Nugent, P.; Belmabkhout, Y.; Burd, S.D.; Cairns, A.J.; Luebke, R.; Forrest, K.; Pham, T.; Ma, S.; Space, B.; Wojtas, L.; et al. Porous materials with optimal adsorption thermodynamics and kinetics for CO<sub>2</sub> separation. *Nature* **2013**, *495*, 80–84. [CrossRef]
16. Xiang, S.; He, Y.; Zhang, Z.; Wu, H.; Zhou, W.; Krishna, R.; Chen, B. Microporous metal-organic framework with potential for carbon dioxide capture at ambient conditions. *Nat. Commun.* **2012**, *3*, 954. [CrossRef]
17. McDonald, T.M.; Mason, J.A.; Kong, X.; Bloch, E.D.; Gygi, D.; Dani, A.; Crocellà, V.; Giordanino, F.; Odoh, S.O.; Drisdell, W.S.; et al. Cooperative insertion of CO<sub>2</sub> in diamine-appended metal-organic frameworks. *Nature* **2015**, *519*, 303–308. [CrossRef]



18. Chen, Q.; Luo, M.; Hammershøj, P.; Zhou, D.; Han, Y.; Laursen, B.W.; Yan, C.-G.; Han, B.-H. Microporous Polycarbazole with High Specific Surface Area for Gas Storage and Separation. *J. Am. Chem. Soc.* **2012**, *134*, 6084–6087. [[CrossRef](#)]
19. Dawson, R.; Stöckel, E.; Holst, J.R.; Adams, D.J.; Cooper, A.I. Microporous organic polymers for carbon dioxide capture. *Energy Environ. Sci.* **2011**, *4*, 4239–4245. [[CrossRef](#)]
20. Shan, M.; Liu, X.; Wang, X.; Yarulina, I.; Seoane, B.; Kapteijn, F.; Gascon, J. Facile manufacture of porous organic framework membranes for precombustion CO<sub>2</sub> capture. *Sci. Adv.* **2018**, *4*, eaau1698. [[CrossRef](#)]
21. Yan, J.; Zhang, B.; Wang, Z. Highly Selective Separation of CO<sub>2</sub>, CH<sub>4</sub>, and C<sub>2</sub>–C<sub>4</sub> Hydrocarbons in Ultramicroporous Semicycloaliphatic Polyimides. *ACS Appl. Mater. Interfaces* **2018**, *10*, 26618–26627. [[CrossRef](#)]
22. Gao, H.; Ding, L.; Bai, H.; Li, L. Microporous Organic Polymers Based on Hyper-Crosslinked Coal Tar: Preparation and Application for Gas Adsorption. *ChemSusChem* **2017**, *10*, 618–623. [[CrossRef](#)]
23. Tan, M.X.; Zhang, Y.; Ying, J. Mesoporous Poly(Melamine-Formaldehyde) Solid Sorbent for Carbon Dioxide Capture. *ChemSusChem* **2013**, *6*, 1186–1190. [[CrossRef](#)]
24. Xu, C.; Hedin, N. Microporous adsorbents for CO<sub>2</sub> capture – a case for microporous polymers? *Mater. Today* **2014**, *17*, 397–403. [[CrossRef](#)]
25. Chaoui, N.; Trunk, M.; Dawson, R.; Schmidt, J.; Thomas, A. Trends and challenges for microporous polymers. *Chem. Soc. Rev.* **2017**, *46*, 3302–3321. [[CrossRef](#)]
26. Rabbani, M.G.; El-Kaderi, H.M. Template-Free Synthesis of a Highly Porous Benzimidazole-Linked Polymer for CO<sub>2</sub> Capture and H<sub>2</sub> Storage. *Chem. Mater.* **2011**, *23*, 1650–1653. [[CrossRef](#)]
27. Lu, W.; Yuan, D.; Sculley, J.; Zhao, D.; Krishna, R.; Zhou, H.-C. Sulfonate-Grafted Porous Polymer Networks for Preferential CO<sub>2</sub> Adsorption at Low Pressure. *J. Am. Chem. Soc.* **2011**, *133*, 18126–18129. [[CrossRef](#)]
28. Xie, L.-H.; Suh, M.P.; Xie, L. High CO<sub>2</sub>-Capture Ability of a Porous Organic Polymer Bifunctionalized with Carboxy and Triazole Groups. *Chem. A Eur. J.* **2013**, *19*, 11590–11597. [[CrossRef](#)]
29. Mohanty, P.; Kull, L.D.; Landskron, K. Porous covalent electron-rich organonitridic frameworks as highly selective sorbents for methane and carbon dioxide. *Nat. Commun.* **2011**, *2*, 401. [[CrossRef](#)]
30. Dawson, R.; Cooper, A.I.; Adams, D.J. Chemical functionalization strategies for carbon dioxide capture in microporous organic polymers. *Polym. Int.* **2013**, *62*, 345–352. [[CrossRef](#)]
31. Haikal, R.R.; Hassan, Y.S.; Emwas, A.-H.; Belmabkhout, Y.; Alkordi, M.H. Poly-functional porous-organic polymers to access functionality—CO<sub>2</sub> sorption energetic relationships. *J. Mater. Chem. A* **2015**, *3*, 22584–22590.
32. Lu, W.; Sculley, J.P.; Yuan, D.; Krishna, R.; Wei, Z.; Zhou, H.-C. Polyamine-Tethered Porous Polymer Networks for Carbon Dioxide Capture from Flue Gas. *Angew. Chem. Int. Ed.* **2012**, *51*, 7480–7484. [[CrossRef](#)]
33. Guillermin, V.; Weselinski, L.J.; Alkordi, M.; Mohideen, M.I.H.; Belmabkhout, Y.; Cairns, A.J.; Eddaoudi, M. Porous organic polymers with anchored aldehydes: A new platform for post-synthetic amine functionalization en route for enhanced CO<sub>2</sub> adsorption properties. *Chem. Commun.* **2014**, *50*, 1937. [[CrossRef](#)]
34. Ratvijitvech, T.; Dawson, R.; Laybourn, A.; Khimiyak, Y.Z.; Adams, D.J.; Cooper, A.I. Post-synthetic modification of conjugated microporous polymers. *Polymer* **2014**, *55*, 321–325. [[CrossRef](#)]
35. Sun, L.-B.; Kang, Y.-H.; Shi, Y.-Q.; Jiang, Y.; Liu, X.-Q. Highly Selective Capture of the Greenhouse Gas CO<sub>2</sub> in Polymers. *ACS Sustain. Chem. Eng.* **2015**, *3*, 3077–3085. [[CrossRef](#)]
36. Puthiaraj, P.; Lee, Y.-R.; Ahn, W.-S. Microporous amine-functionalized aromatic polymers and their carbonized products for CO<sub>2</sub> adsorption. *Chem. Eng. J.* **2017**, *319*, 65–74. [[CrossRef](#)]
37. Xu, C.; Bacsik, Z.; Hedin, N. Adsorption of CO<sub>2</sub> on a micro-/mesoporous polyimine modified with tris(2-aminoethyl)amine. *J. Mater. Chem. A* **2015**, *3*, 16229–16234. [[CrossRef](#)]
38. Sung, S.; Suh, M.P. Highly efficient carbon dioxide capture with a porous organic polymer impregnated with polyethylenimine. *J. Mater. Chem. A* **2014**, *2*, 13245–13249. [[CrossRef](#)]
39. Lu, W.; Sculley, J.P.; Yuan, D.; Krishna, R.; Zhou, H.-C. Carbon Dioxide Capture from Air Using Amine-Grafted Porous Polymer Networks. *J. Phys. Chem. C* **2013**, *117*, 4057–4061. [[CrossRef](#)]
40. Hedin, N.; Andersson, L.; Bergström, L.; Yan, J. Adsorbents for the post-combustion capture of CO<sub>2</sub> using rapid temperature swing or vacuum swing adsorption. *Appl. Energy* **2013**, *104*, 418–433. [[CrossRef](#)]
41. Xu, Y.; Jin, S.; Xu, H.; Nagai, A.; Jiang, D. Conjugated microporous polymers: Design, synthesis and application. *Chem. Soc. Rev.* **2013**, *42*, 8012. [[CrossRef](#)]

42. Ben, T.; Ren, H.; Ma, S.; Cao, D.; Lan, J.; Jing, X.; Wang, W.; Xu, J.; Deng, F.; Simmons, J.M.; et al. Targeted Synthesis of a Porous Aromatic Framework with High Stability and Exceptionally High Surface Area. *Angew. Chem. Int. Ed.* **2009**, *48*, 9457–9460. [[CrossRef](#)]
43. Sprick, R.S.; Jiang, J.-X.; Bonillo, B.; Ren, S.; Ratvijitvech, T.; Guiglion, P.; Zwijnenburg, M.A.; Adams, D.J.; Cooper, A.I. Tunable Organic Photocatalysts for Visible-Light-Driven Hydrogen Evolution. *J. Am. Chem. Soc.* **2015**, *137*, 3265–3270. [[CrossRef](#)]
44. Chen, L.; Honsho, Y.; Seki, S.; Jiang, D. Light-Harvesting Conjugated Microporous Polymers: Rapid and Highly Efficient Flow of Light Energy with a Porous Polyphenylene Framework as Antenna. *J. Am. Chem. Soc.* **2010**, *132*, 6742–6748. [[CrossRef](#)]
45. Jiang, J.-X.; Su, F.; Niu, H.; Wood, C.D.; Campbell, N.L.; Khimyak, Y.Z.; Cooper, A.I. Conjugated microporous poly(phenylene butadiynylene)s. *Chem. Commun.* **2008**, 486–488. [[CrossRef](#)]
46. Jiang, J.-X.; Su, F.; Trewin, A.; Wood, C.D.; Campbell, N.L.; Niu, H.; Dickinson, C.; Ganin, A.Y.; Rosseinsky, M.J.; Khimyak, Y.Z.; et al. Conjugated Microporous Poly(aryleneethynylene) Networks. *Angew. Chem. Int. Ed.* **2007**, *46*, 8574–8578. [[CrossRef](#)]
47. Choi, J.; Ko, J.H.; Kang, C.W.; Lee, S.M.; Kim, H.J.; Ko, Y.-J.; Yang, M.; Son, S.U. Enhanced redox activity of a hollow conjugated microporous polymer through the generation of carbonyl groups by carbonylative Sonogashira coupling. *J. Mater. Chem. A* **2018**, *6*, 6233–6237. [[CrossRef](#)]
48. Karabiyikoglu, S.; Kelgokmen, Y.; Zora, M. Facile synthesis of iodopyridines from N-propargylic  $\beta$ -enaminones via iodine-mediated electrophilic cyclization. *Tetrahedron* **2015**, *71*, 4324–4333. [[CrossRef](#)]
49. Kelgokmen, Y.; Zora, M. Facile synthesis of heavily-substituted alkynylpyridines via a Sonogashira approach. *RSC Adv.* **2016**, *6*, 4608–4621. [[CrossRef](#)]
50. Hoven, B.G.V.D.; Alper, H. Innovative Synthesis of 4-Carbaldehydepyrrolin-2-ones by Zwitterionic Rhodium Catalyzed Chemo- and Regioselective Tandem Cyclohydrocarbonylation/CO Insertion of  $\alpha$ -Imino Alkynes. *J. Am. Chem. Soc.* **2001**, *123*, 10214–10220. [[CrossRef](#)]
51. Waldo, J.P.; LaRock, R.C. The Synthesis of Highly Substituted Isoxazoles by Electrophilic Cyclization. An Efficient Synthesis of Valdecoxib. *J. Org. Chem.* **2007**, *72*, 9643–9647. [[CrossRef](#)]
52. Liu, X.; Hong, D.; She, Z.; Hersh, W.H.; Yoo, B.; Chen, Y. Complementary regioselective synthesis of 3,5-disubstituted isoxazoles from ynones. *Tetrahedron* **2018**, *74*, 6593–6606. [[CrossRef](#)]
53. Socrates, G. *Infrared and Raman Characteristic Group Frequencies: Tables and Charts*; John Wiley & Sons: Hoboken, NJ, USA, 2004.
54. Xu, C.; Hedin, N. Synthesis of microporous organic polymers with high CO<sub>2</sub>-over-N<sub>2</sub> selectivity and CO<sub>2</sub> adsorption. *J. Mater. Chem. A* **2013**, *1*, 3406. [[CrossRef](#)]
55. Bacsik, Z.; Atluri, R.; Garcia-Bennett, A.E.; Hedin, N. Temperature-Induced Uptake of CO<sub>2</sub> and Formation of Carbamates in Mesocaged Silica Modified with n-Propylamines. *Langmuir* **2010**, *26*, 10013–10024. [[CrossRef](#)]
56. Knoöfel, C.; Martin, C.; Hornebecq, V.; Llewellyn, P.L. Study of Carbon Dioxide Adsorption on Mesoporous Aminopropylsilane-Functionalized Silica and Titania Combining Microcalorimetry and in Situ Infrared Spectroscopy. *J. Phys. Chem. C* **2009**, *113*, 21726–21734.
57. Danon, A.; Stair, P.C.; Weitz, E. FTIR Study of CO<sub>2</sub> Adsorption on Amine-Grafted SBA-15: Elucidation of Adsorbed Species. *J. Phys. Chem. C* **2011**, *115*, 11540–11549. [[CrossRef](#)]
58. Aziz, B.; Hedin, N.; Bacsik, Z. Quantification of chemisorption and physisorption of carbon dioxide on porous silica modified by propylamines: Effect of amine density. *Micropor. Mesopor. Mater.* **2012**, *159*, 42–49. [[CrossRef](#)]
59. Fu, F.-N.; DeOliveira, D.B.; Trumble, W.R.; Sarkar, H.K.; Singh, B.R. Secondary Structure Estimation of Proteins Using the Amide III Region of Fourier Transform Infrared Spectroscopy: Application to Analyze Calcium-Binding-Induced Structural Changes in Calsequestrin. *Appl. Spectrosc.* **1994**, *48*, 1432–1441. [[CrossRef](#)]
60. Wang, X.; Schwartz, V.; Clark, J.C.; Ma, X.; Overbury, S.H.; Xu, X.; Song, C. Infrared Study of CO<sub>2</sub> Sorption over “Molecular Basket” Sorbent Consisting of Polyethylenimine-Modified Mesoporous Molecular Sieve. *J. Phys. Chem. C* **2009**, *113*, 7260–7268. [[CrossRef](#)]
61. Hiyoshi, N.; Yogo, K.; Yashima, T. Adsorption characteristics of carbon dioxide on organically functionalized SBA-15. *Micropor. Mesopor. Mater.* **2005**, *84*, 357–365. [[CrossRef](#)]

62. Bacsik, Z.; Ahlsten, N.; Ziadi, A.; Zhao, G.; Garcia-Bennett, A.E.; Martín-Matute, B.; Hedin, N. Mechanisms and Kinetics for Sorption of CO<sub>2</sub> on Bicontinuous Mesoporous Silica Modified with n-Propylamine. *Langmuir* **2011**, *27*, 11118–11128. [[CrossRef](#)]
63. Huang, H.Y.; Yang, R.T.; Chinn, D.; Munson, C.L. Amine-Grafted MCM-48 and Silica Xerogel as Superior Sorbents for Acidic Gas Removal from Natural Gas. *Ind. Eng. Chem. Res.* **2003**, *42*, 2427–2433. [[CrossRef](#)]
64. Myers, A.L.; Prausnitz, J.M. Thermodynamics of mixed-gas adsorption. *AIChE J.* **1965**, *11*, 121–127. [[CrossRef](#)]
65. Patel, H.H.A.; Byun, J.; Yavuz, C.T. Carbon Dioxide Capture Adsorbents: Chemistry and Methods. *ChemSusChem* **2017**, *10*, 1303–1317. [[CrossRef](#)] [[PubMed](#)]
66. McDonald, T.M.; D'Alessandro, D.M.; Krishna, R.; Long, J.R. Enhanced carbon dioxide capture upon incorporation of N,N'-dimethylethylenediamine in the metal-organic framework CuBTTri. *Chem. Sci.* **2011**, *2*, 2022–2028. [[CrossRef](#)]
67. Choi, S.; Gray, M.L.; Jones, C.W. Amine-Tethered Solid Adsorbents Coupling High Adsorption Capacity and Regenerability for CO<sub>2</sub> Capture from Ambient Air. *ChemSusChem* **2011**, *4*, 628–635. [[CrossRef](#)] [[PubMed](#)]



© 2019 by the authors. Licensee MDPI, Basel, Switzerland. This article is an open access article distributed under the terms and conditions of the Creative Commons Attribution (CC BY) license (<http://creativecommons.org/licenses/by/4.0/>).